RNA (2000), *6*:744–754. Cambridge University Press. Printed in the USA.

Puromycin–rRNA interaction sites at the peptidyl transferase center

CRISTINA RODRIGUEZ-FONSECA,[1,2] HIEN PHAN,[1] KATHERINE S. LONG,[1] BO T. PORSE,[1] STANISLAV V. KIRILLOV,[3] RICARDO AMILS,[2] and ROGER A. GARRETT[1]

[1]RNA Regulation Centre, Institute of Molecular Biology, University of Copenhagen, Sølvgade 83H, DK-1307 Copenhagen K, Denmark
[2]Centro de Biología Molecular, Universidad Autónoma de Madrid, Campus de Cantoblanco, E-28049 Madrid, Spain
[3]Petersburg Nuclear Physics Institute, Russian Academy of Sciences, 188350 Gatchina, St. Petersburg, Russia

ABSTRACT

The binding site of puromycin was probed chemically in the peptidyl-transferase center of ribosomes from *Escherichia coli* and of puromycin-hypersensitive ribosomes from the archaeon *Haloferax gibbonsii.* Several nucleotides of the 23S rRNAs showed altered chemical reactivities in the presence of puromycin. They include A2439, G2505, and G2553 for *E. coli,* and G2058, A2503, G2505, and G2553 for *Hf. gibbonsii* (using the *E. coli* numbering system). Reproducible enhanced reactivities were also observed at A508 and A1579 within domains I and III, respectively, of *E. coli* 23S rRNA. In further experiments, puromycin was shown to produce a major reduction in the UV-induced crosslinking of deacylated-(2N_3A76)tRNA to U2506 within the P′ site of *E. coli* ribosomes. Moreover, it strongly stimulated the putative UV-induced crosslink between a streptogramin B drug and m^2A2503/Ψ2504 at an adjacent site in *E. coli* 23S rRNA. These data strongly support the concept that puromycin, along with other peptidyl-transferase antibiotics, in particular the streptogramin B drugs, bind to an RNA structural motif that contains several conserved and accessible base moieties of the peptidyl transferase loop region. This streptogramin motif is also likely to provide binding sites for the 3′ termini of the acceptor and donor tRNAs. In contrast, the effects at A508 and A1579, which are located at the exit site of the peptide channel, are likely to be caused by a structural effect transmitted along the peptide channel.

Keywords: 23S rRNA; peptide channel; peptidyl transferase; puromycin

INTRODUCTION

The antibiotic puromycin has played a central role in our understanding of the mechanism of peptide elongation in the ribosome. This is because it is partially costructural with the 3′ terminus of aminoacyl-tRNA (Harris & Symons, 1973) (Fig. 1) and can, therefore, function as an amino acid acceptor substrate (Traut & Monro, 1964; Smith et al., 1965). This property of the drug has been exploited in assays for peptide-bond formation and elongation. These have yielded important, albeit superficial, insight into the mechanisms of inhibition of peptide-bond formation by many other antibiotics (reviewed in Pestka, 1977; Vázquez, 1979; Gale et al., 1981).

Reprint requests to: Professor R.A. Garrett, RNA Regulation Centre, Institute of Molecular Biology, University of Copenhagen, Sølvgade 83H, DK-1307 Copenhagen K, Denmark; e-mail: garrett@mermaid.molbio.ku.dk.

Several antibiotics have been footprinted on free ribosomes within the peptidyl-transferase loop of 23S rRNA, including some that bind competitively with puromycin (reviewed in Garrett & Rodriguez-Fonseca, 1995). Moreover, for some of the antibiotics, but not puromycin, drug-resistant mutants have been isolated from bacteria and haloarchaea that carry single-site mutations in the peptidyl-transferase loop (Garrett & Rodriguez-Fonseca, 1995). This, together with recent UV-induced crosslinking data for sparsomycin (Porse et al., 1999b) and for the streptogramin B, pristinamycin IA (Porse et al., 1999a), within this rRNA region suggest that most, if not all, peptidyl-transferase antibiotics bind there (reviewed in Porse et al., 2000).

Localization of the puromycin-binding site is important for defining the position of the 3′ end of aminoacyl-tRNA immediately prior to peptide-bond formation (Porse et al., 1995; Kirillov et al., 1997). However, these experiments are difficult to execute for several reasons. First, puromycin binds very weakly to

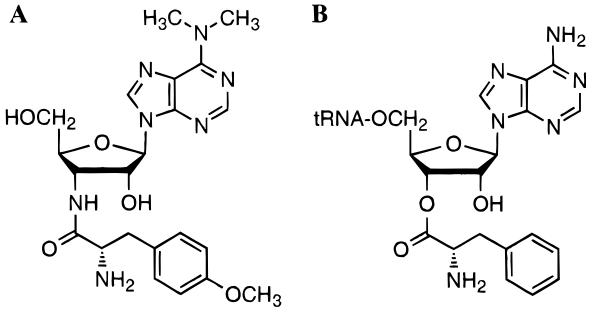

FIGURE 1. Chemical structures of **A**: puromycin, and **B**: the 3′-end of a phenylalanyl-tRNA molecule.

free ribosomes (Pestka, 1970; Fernandez-Muñoz & Vázquez, 1973). In addition, because the drug is an analog of the aminoacyl-acceptor substrate, it is also a potential analog of the donor substrate, and may therefore bind weakly in the P′ site (Kirillov et al., 1997) of free ribosomes (Bourd et al., 1983). Furthermore, probing in the presence of an active donor substrate will result in peptide bond formation, which will occur coincidentally with the probable movement of the puromycin-peptide complex (Odom et al., 1990).

Several crosslinking investigations with different puromycin derivatives have provided useful information on the location of the puromycin-binding site. In one experiment, the derivative [^{3}H]-*p*-azidopuromycin was bound to free ribosomes and, upon irradiation with UV light, crosslinked to positions G2502 and U2504, at the base of the peptidyl-transferase loop. The derivative was also crosslinked to protein L23, which binds to domain III of 23S rRNA (Nicholson et al., 1982a, 1982b; Hall et al., 1988). In another experiment, an attempt was made to locate the equivalent of C-74 of aminoacyl-tRNA by attaching an affinity label to puromycin (Green et al., 1998). A crosslink was produced to position 2553 outside of the peptidyl-transferase loop, some 10 Å from the acceptor group of puromycin. Only in the latter experiment was evidence provided for the derivatized puromycin occupying a functional acceptor-substrate site.

In the present work, three strategies are used to locate the puromycin-binding site and its effects on 23S rRNA. First, an rRNA-footprinting approach was employed on puromycin complexed with ribosomes from *Escherichia coli* and the haloarchaeon *Haloferax gibbonsii*. The latter ribosomes were included to provide complementary data from another domain of life and, moreover, they are hypersensitive to puromycin (Sanz et al., 1993). Second, a study was made of the effect of puromycin on the crosslinking of deacylated-(2N_3A76) tRNA bound to the P′ site of 70S ribosome–poly(U) complexes. Finally, the effect of puromycin on the putative UV-induced crosslinking of pristinamycin IA within the peptidyl-transferase loop of 23S rRNA was examined.

RESULTS

In vitro rRNA footprinting of puromycin complexed to *E. coli* and *Hf. gibbonsii* ribosomes

Puromycin–ribosome complexes were formed by incubating ribosomes from *E. coli* (Makhno et al., 1988) and *Hf. gibbonsii* with increasing concentrations of puromycin (0.1, 0.5, 1, 2, and 4 mM). The complexes and control samples of free ribosomes were then treated with the base-specific reagents dimethylsulfate (DMS) [G (N-7) > A (N-1) > C (N-3)], kethoxal [G (N-1, N-2)], and CMCT (1-cyclohexyl-3(2-morpholinoethyl)-carbodiimide metho-p-toluene sulfonate) [U (N-3) > G (N-1)]. After removal of excess reagent and proteins, deoxyoligonucleotide primers were hybridized to 23S rRNA, 3′ from the RNA region to be investigated, subjected to primer extension, and analyzed on polyacrylamide sequencing gels.

The most extensive work was done on *E. coli* ribosomes where we studied puromycin complexes systematically with 70S ribosomes, 50S subunits, and with polysomes, and for each of the complexes, the whole range of puromycin concentrations was tested. Moreover, puromycin aminonucleoside was included in all of these experiments in the concentration range 0.1 to 2 mM as a control. For the halophile ribosomes, only puromycin complexes with 70S ribosomes were examined. For the 70S ribosomes of both organisms, altered nucleotide reactivities, including protections and enhancements, were observed. Puromycin-induced effects were not detected at the lowest puromycin concentration (0.1 mM), in accordance with an earlier observation for *E. coli* ribosomes, which was attributed to the low binding constant of puromycin (Moazed & Noller, 1987). Autoradiograms of gels illustrating some of the changes for DMS- and kethoxal-modified samples, including control samples modified in the absence of antibiotics for *E. coli* and *Hf. gibbonsii*, are depicted in Figures 2 and 3, respectively. No reactivity changes were observed for CMCT-modified samples.

Reactivity changes were quantified by microdensitometry relative to adjacent control bands. Representative scans are illustrated for the reactions at positions A508 and G2505 at different puromycin concentrations in Figure 4. All the effects are summarized in Table 1, where horizontally aligned nucleotides occur at corresponding positions in the two secondary structures of 23S rRNA (Figs. 5 and 6). The intensity changes between 0 and 2 mM puromycin, for all of the nucleotides, were in the range 30–70%. There is no reason to expect that the total intensity change should be similar for the different nucleotides, as in total they represent differences in the accessibility of two chemicals at various positions in the ribosome in the presence of puromycin.

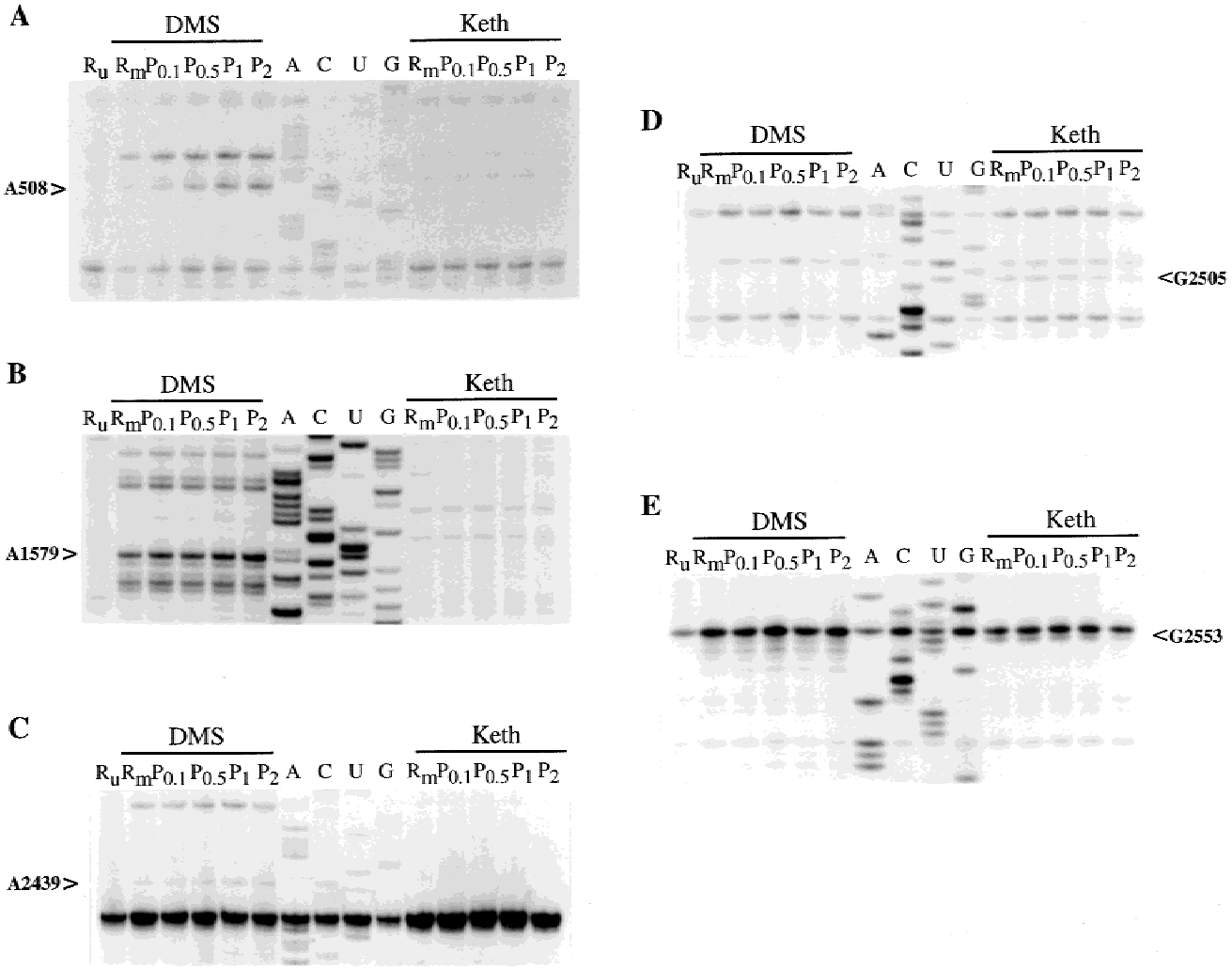

FIGURE 2. Autoradiograms showing puromycin-induced changes in nucleotide reactivities of 23S rRNA isolated from 70S ribosomes of *E. coli*. Altered reactivities are indicated with arrows. 70S ribosomes and their complexes with puromycin were modified with DMS or kethoxal (Keth). Unmodified ribosomes (R_u), ribosomes modified in the absence of drug (R_m), and ribosomes modified in the presence of puromycin (P—0.1, 0.5, 1, or 2 mM) were coelectrophoresed in the different experiments. Identical changes in the modification patterns were also observed for puromycin complexes with 50S subunits and with polysomes. Lanes A, C, G, and U represent dideoxy-sequencing reactions. The reverse transcription termination effects are offset by one residue from the corresponding positions in the sequencing tracks.

Most of the altered reactivities were localized in, or adjoining, the peptidyl-transferase loop of domain V (Fig. 5). This domain, together with domain IV, was screened many times (>20) for altered nucleotide reactivities in both organisms. The remainder of *E. coli* 23S rRNA was screened at least twice, and reproducible enhanced reactivities were observed in domain I (Fig. 6A) and domain III (Fig. 6B). The remainder of the extreme halophile 23S rRNA was also screened, but additional altered nucleotide reactivities were not observed.

Similar protection effects were observed for both organisms at nt G2505 (Figs. 2D, 3B, and 4B) and G2553 (Fig. 2E), using *E. coli* numbering (Table 1). However, effects were also detected that were particular to each organism. In *E. coli*, enhanced reactivities were seen at A2439 (Fig. 2C), in addition to A508 (Figs. 2A and 4A) and A1579 (Fig. 2 B), in domains I and III, respectively. Reactivity changes in *Hf. gibbonsii* were observed at G2058 (G2084) (Fig. 3A) and A2503 (A2521) (Fig. 3B), that correspond in identity to A2058 and m^2A2503, respectively, in *E. coli*. In vitro footprinting experiments were also carried out systematically on 70S ribosomes of another extreme halophile, *Hf. mediterranei*. Both halophiles yielded indistinguishable results (data not shown) for the effects summarized in Table 1, that did not reflect the 3.5-fold higher sensitivity of the *Hf. gibbonsii* ribosomes to puromycin measured in in vitro assays (Sanz et al., 1993).

Variable reactivity changes were observed at position 2062 in both *E. coli* and the haloarchaeal ribosomes. These weak effects are not included in Table 1 because not all of the criteria for significance (outlined in Materials and methods) were met. A weak enhance-

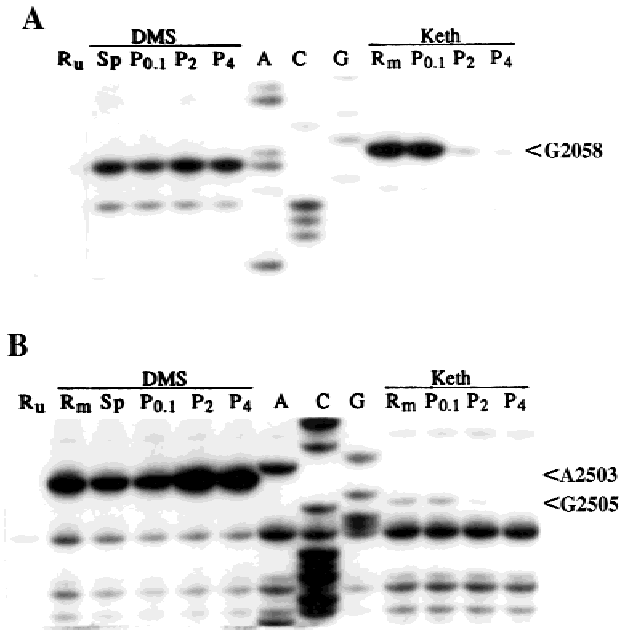

FIGURE 3. Selected puromycin-induced changes in nucleotide reactivities in 23S rRNA isolated from *Hf. gibbonsii.* Altered reactivities G2058 (G2084), A2059 (A2085), A2503 (A2521), and G2505 (G2523) are indicated with arrows. 70S ribosomes and their complexes with puromycin were modified with DMS or Keth. Unmodified ribosomes (R_u), ribosomes modified in the absence of drug (R_m), and ribosomes modified in the presence of puromycin (P—0.1, 2, or 4 mM) were coelectrophoresed in the different experiments. The lanes labeled Sp are a reaction with ribosomes modified in the presence of sparsomycin (1 mM), included as a negative control. Lanes A, C, G, and U represent dideoxy-sequencing reactions. The reverse transcription termination effects are offset by one residue from the corresponding positions in the sequencing tracks.

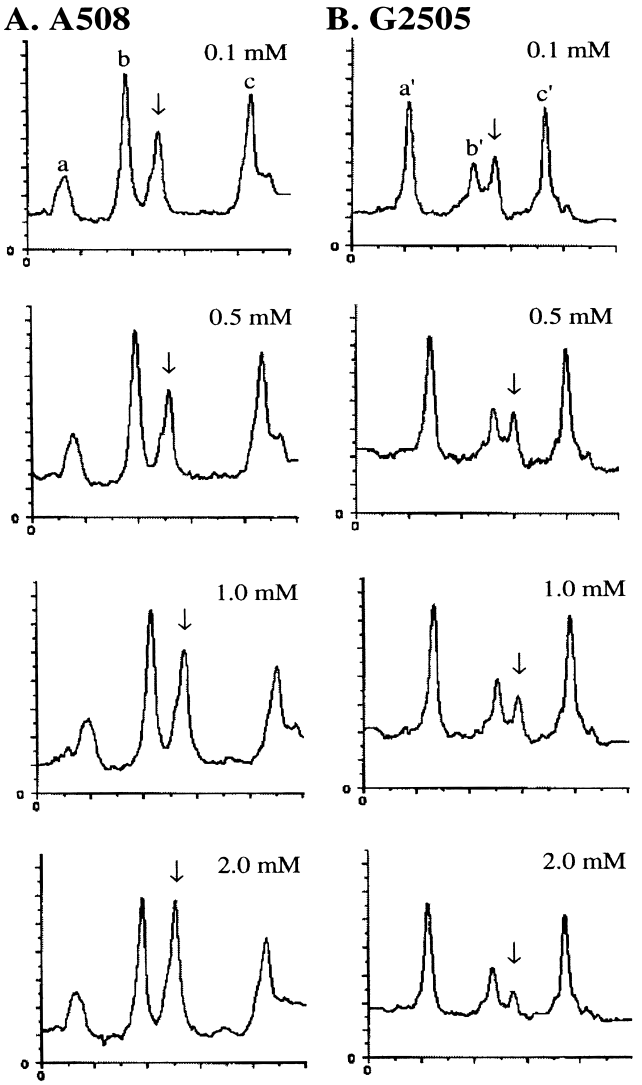

FIGURE 4. Microdensitometry scans illustrating the effects at A508 and G2505 over a 0.1–2.0 mM puromycin-concentration range. The plots represent portions of scanned autoradiogram lanes, with the ordinate and abscissa in arbitrary units of signal intensity and length, respectively. Peaks showing enhancement at A508 (**A**) and protection at G2505 (**B**) are indicated with arrows. The labeled control bands are G496 (a), A504 (b), G518 (c), A2497 (a′), A2503 (b′), and C2510 (c′). The intensity change at a given position was calculated using the peak heights with a subtracted baseline correction for each peak. The total changes in peak intensity for A508 and G2505 were 44% and 52%, respectively. The scans at 0.1 mM puromycin were indistinguishable from those of samples with no puromycin added.

ment was observed at 2062 of *E. coli* relative to the effects at A2058 and A2059 that could not be quantified because of the lack of strong adjacent control bands. Moreover, a very weak protection effect was observed at 2062 for the extreme halophiles (Fig. 3A).

The *E. coli* experiments were also done on 50S subunits and polysomes, and for the latter, two types of experiments were performed. In one, a mixture of polysome peaks was isolated from a gradient before the addition of puromycin and chemical modification. In the other, the samples were rerun on a gradient, after incubation with puromycin and chemical modification, and the stable polysome peaks were again pooled and precipitated. For each of the ribosomal complexes, the patterns of altered reactivities were indistinguishable from those of the 70S ribosomal particles (Fig. 2; Table 1). In all of these experiments, puromycin aminonucleoside was included, which is an analog of puromycin with an amino group replacing the modified aminoacyl group at the 3′ position. No altered reactivities were detected in the 23S rRNAs of any of the *E. coli* ribosomal particles (data not shown). Control footprinting experiments were also carried out on mixtures of puromycin and free 23S rRNA for *E. coli*, and on puromycin complexes with *E. coli* ribosomes from which the 5S rRNA was subsequently extracted and examined for chemical modification. No altered nucleotide reactivities were observed at a puromycin concentration of 2 mM.

Effect of puromycin on the crosslinking of a P-site bound tRNA substrate

It has been demonstrated that tRNA substrates substituted with an azido group at the 2 position of the 3′-

TABLE 1. Nucleotide positions exhibiting altered reactivities in the presence of 0 and 2 mM puromycin within *E. coli* and *Hf. gibbonsii* 23S rRNAs.

	E. coli		*Hf. gibbonsii*	
Nucleotide	− puromycin	+ puromycin	− puromycin	+ puromycin
A508	+	++		
A1579	+	++		
A2058 (G2084)			++	(+)
A2439 (A2458)	(+)	+		
m^2A2503 (A2521)			++	+++
G2505 (G2523)	+	(+)	(+)	−
G2553 (G2571)	+	(+)	+	(+)

The intensities of the autoradiographed bands were quantified by microdensitometry and are denoted as: +++ strong, ++ medium, + weak, and (+) very weak. Intensities were assigned through visual inspection of several sets of films in combination with microdensitometry. The total intensity changes summarized above represent minimum total intensity changes of 25–30% (see legend to Fig. 4 and Materials and methods). The total percentage changes observed for *E. coli* ribosomes, between 0 and 2 mM puromycin, were A508 (44%), A1579 (71%), A2439 (37%), G2505 (52%), and G2553 (32%). Error limits were estimated at ±10% of the number given. Experiments were performed with 70S ribosomes, from which 23S rRNA was isolated (see Materials and methods). For *E. coli*, similar reactivity changes were observed with 50S subunits and polysomes. Nucleotide positions are given using *E. coli* 23S rRNA numbering (Egebjerg et al., 1990), with the corresponding *H. halobium* numbering given in parentheses.

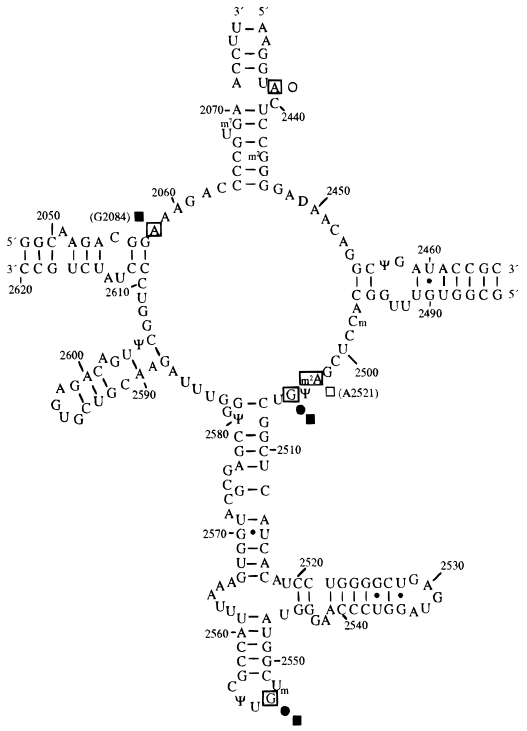

FIGURE 5. The location of puromycin-induced effects in the peptidyltransferase loop and adjoining regions of domain V of 23S rRNA. The sequence shown is that of *E. coli* 23S rRNA. Nucleotides affected by puromycin in *E. coli* and *Hf. gibbonsii* 23S rRNAs are boxed and labeled. Altered reactivities are indicated with circles and squares, for *E. coli* and *Hf. gibbonsii*, respectively. Protections are denoted with filled symbols, whereas open symbols indicate enhancements. Where corresponding nucleotides in the two rRNAs differ, the identity and numbering of the halophile nucleotide is given in parentheses. Nucleotides joined by lines are base paired, and posttranscriptional modifications are indicated (Smith et al., 1992).

terminal adenosine residue, and bound at the ribosomal P-site, generate crosslinks with 23S rRNA and ribosomal proteins L27 and L33 upon UV irradiation at 365 nM (Wower et al., 1995). The RNA crosslinks have been localized on previously characterized 23S rRNA fragments F1′, F2′, and F4′ at nt C2601/A2602 and U2584/U2585 (F1′), U2506 (F2′), and A2062/C2063 (F4′) (Kirillov et al., 1999). Puromycin was tested for its ability to alter the yields or identities of these crosslinks. It was added to 70S ribosome-poly (U) complexes before addition of azidoadenosine tRNA substrate and irradiation. Unlike experiments performed with other antibiotics (Kirillov et al., 1999), those with puromycin were done only in the presence of deacylated tRNA substrate. The use of an active peptidyl-tRNA donor substrate was avoided, as this, in conjunction with puromycin, would complicate the interpretation of results owing to peptide-bond formation and the subsequent dissociation of peptidyl-puromycin.

Puromycin did not change the level of tRNA binding to the ribosome, but it did produce significant decreases in crosslinking yields at two of three rRNA sites. In addition, no new crosslinks were detected with puromycin. The changes in crosslinking yields for each rRNA fragment are depicted in Figure 7 and the quantified yields are summarized in Table 2. In the presence of the drug, no crosslink was formed with F4′, and the crosslink to F2′ was reduced by about 50%. The crosslink to F1′ was not significantly affected by puromycin averaged over four independent experiments (Table 2). Moreover, no significant changes in the crosslinking yields to ribosomal proteins were observed in the presence of the drug (data not shown).

Effect of puromycin on pristinamycin IA-dependent rRNA modifications

The streptogramin B drug pristinamycin IA produces modifications in *E. coli* 23S rRNA at m^2A2503/Ψ2504 and G2061/A2062 upon irradiation with 365 nM light, where the former sites, at least, are likely to involve a drug–rRNA crosslink (Porse et al., 1999a). Given the proximity of the footprinting sites to m^2A2503/Ψ2504, the ability of puromycin to influence these pristinamycin IA-dependent rRNA modifications was investigated (Fig. 8). Puromycin was added to a preformed complex of pristinamycin IA and 70S ribosome–poly (U) complexes before irradiating and analyzing the peptidyltransferase-loop region by primer extension. Puromycin enhanced the pristinamycin IA-dependent reverse transcriptase stops at m^2A2503/Ψ2504 by 2.5-fold (Fig. 8, lanes 2 and 3), but had no detectable effect on those at

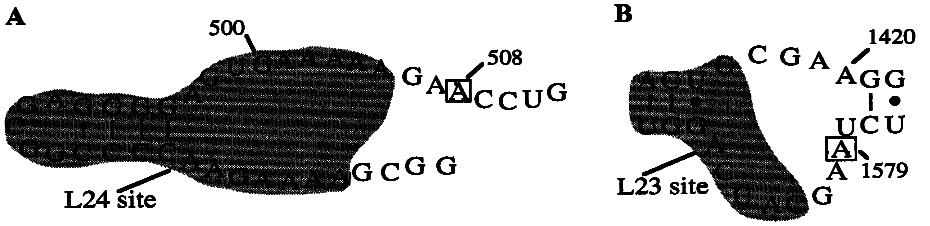

FIGURE 6. Putative allosteric effects dependent on puromycin in domains I and III of *E. coli* 23S rRNA. Nucleotides exhibiting enhanced reactivities in the presence of puromycin are boxed in (**A**) domain I and (**B**) domain III. The shaded regions are binding sites for ribosomal proteins L24 (Egebjerg et al., 1987) and L23 (Egebjerg et al., 1991).

G2061/A2062 (data not shown). Control experiments in which the order of drug addition was reversed yielded identical results (data not shown). The yields of the rRNA modifications were enhanced another twofold in the presence of both drugs with a P-site bound deacylated $tRNA^{Phe}$ substrate (Fig. 8, lanes 5 and 6). This is consistent with deacylated tRNA producing a threefold increase in the pristinamycin IA-dependent modification yields at $m^2A2503/\Psi2504$ (Porse et al., 1999a). Moreover, the puromycin-induced enhancement of the PIA modification in both the presence and absence of a P-site bound tRNA suggests that puromycin resides in the A-site in both ribosomal complexes.

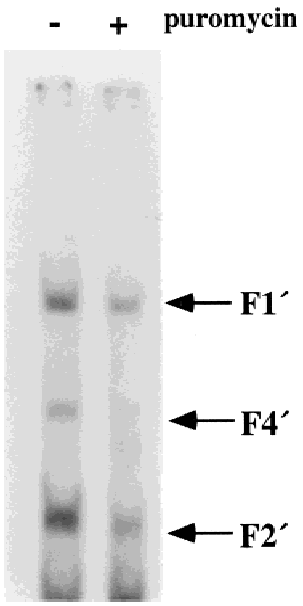

FIGURE 7. The effect of puromycin on the crosslinking yields of deacylated $(2N_3A76)tRNA^{Phe}$, bound at the ribosomal P site, to fragments of 23S rRNA. Complexes were prepared in the absence (control) or presence of puromycin (1 mM), before binding of $[^{32}P](2N_3A76)tRNA^{Phe}$ and irradiation (see Materials and methods). The specific activity of $[^{32}P](2N_3A76)tRNA^{Phe}$ was 3,000 dpm/pmol. The crosslinked fragments were generated by RNase H digestion with a set of deoxyoligonucleotides (see Materials and methods), and analyzed on polyacrylamide gels. The positions of the three main labeled fragments F1′, F2′, and F4′ are indicated. Although the intensity of the F1′ crosslink appears reduced in the puromycin lane, when the counts are adjusted for the degree of tRNA binding to ribosomes, the differences are minimal (Table 2).

DISCUSSION

For both the bacterial and archaeal ribosomes, most of the puromycin-induced effects lie within, or adjacent to, the peptidyl-transferase loop of domain V of 23S rRNA (Fig. 9). Of these effects, all except one are at universally conserved nucleotides, which is consistent with puromycin-inhibiting bacterial, archaeal, and eukaryotic ribosomes. Moreover, the fact that the effects appeared within the same concentration range suggests that they derive from a single drug-binding site.

The protection effects common to *E. coli* and *Hf. gibbonsii* occur at the universally conserved nt G2505 and G2553. G2505 is the site of altered nucleotide reactivity in the presence of several other antibiotics, including the macrolides carbomycin and tylosin, and the streptogramin A drugs (Garrett & Rodriguez-Fonseca, 1995; Porse & Garrett, 1999). In a recent investigation, G2553 was specifically crosslinked to the A-site tRNA analog, 4-thio-dT-p-C-p-puromycin (Green et al., 1998). In another study, all possible mutations made at G2553 in *E. coli* resulted in dominant growth defects in vivo, as well as reduced peptidyl transferase activity in vitro (Kim & Green, 1999). In addition, complementation analysis of mutant A-site substrate analogs and ribosomes established a specific interaction between C75 of the aminoacyl–tRNA and G2553 of 23S rRNA (Kim & Green, 1999). An important role for this rRNA loop in puromycin binding is also suggested by mutagenesis and damage-selection experiments, in which changes at 2550, 2552, 2555, and 2557 interfered with the transfer

TABLE 2. Summary of the crosslinking yields of deacylated $(2N_3A76)tRNA^{Phe}$ to rRNA fragments F1′, F2′, and F4′.

Antibiotic	F1′	F2′	F4′
none	13 ± 2	25 ± 3	7 ± 1
puromycin	10 ± 1	13 ± 2	n.b.[a]

Data are presented as counts per minute of crosslinked deacylated $(2N_3A76)tRNA^{Phe}$ per picomole of ribosome-bound deacylated $(2N_3A76)tRNA^{Phe}$. The specific activity of the $(2N_3A76)tRNA^{Phe}$ was normalized to an initial activity of 10,000 dpm/pmol or about 1,800 cpm/pmol estimated in an Instant Imager. The data were averaged from four separate experiments.

[a] n.b.: no band detected.

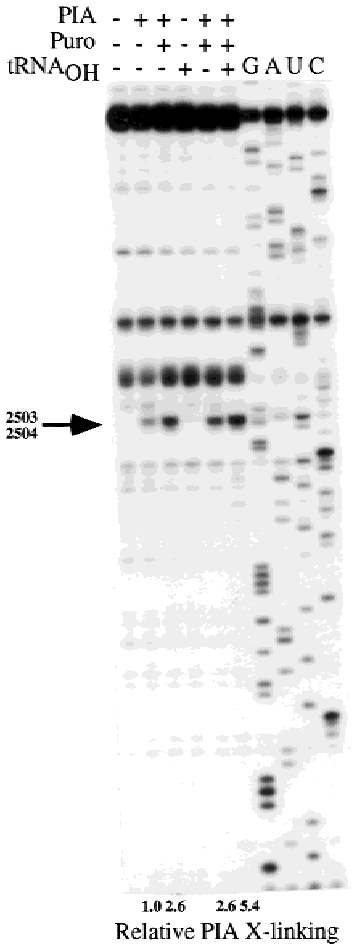

FIGURE 8. The effect of puromycin (puro) on UV-induced modifications of *E. coli* 70S ribosomes that are dependent on pristinamycin IA (PIA). Pristinamycin IA (10 μM) was complexed to 70S ribosome (0.15 μM) –poly(U) complexes in the absence or presence of deacylated tRNA and was incubated at 37 °C for 10 min. Puromycin (1 mM) was added and incubation was continued for 10 min. The samples were then irradiated at 365 nM for 20 min. Primer extension analyses were performed by using EC2621 (5′-CAGTTCTCCAGC GCCCAC-3′), a primer complementary to positions 2638–2621 of *E. coli* 23S rRNA. The primer extension stops at 2503 and 2504 were quantified in an Instant Imager, using the stop at 2497 as a reference, and the results are shown below the gel, relative to a control sample in the absence of puromycin. G, A, U, and C represent dideoxy-sequencing reactions.

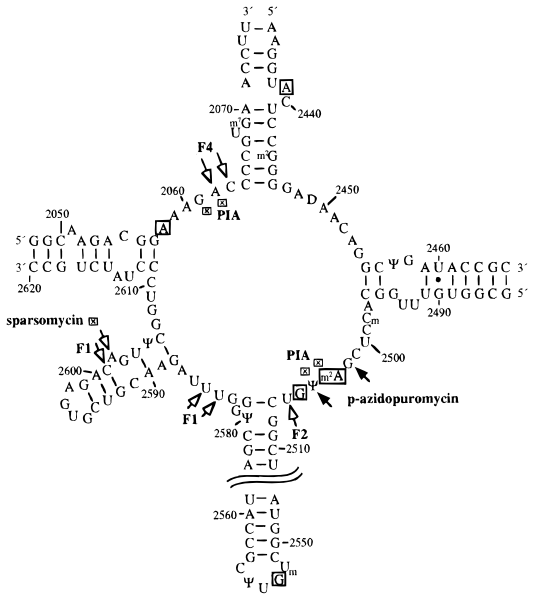

FIGURE 9. Summary of the puromycin effects in the peptidyl-transferase loop of 23S rRNA. The sites of altered nucleotide reactivities for *E. coli* and *Hf. gibbonsii* are boxed on the *E. coli* 23S rRNA sequence (see Fig. 5). Sites of drug-dependent UV-induced crosslinks or modifications are labelled with boxed crosses. The sites of crosslinks with P-site bound tRNA substrate are denoted with open-headed arrows. Filled arrows indicate sites of crosslinking with p-azidopuromycin.

of peptidyl moiety to puromycin (Porse & Garrett, 1995; Bocchetta et al., 1998). Taken together, the data suggest that the loop containing G2553 folds into the catalytic center and is in close proximity with the 3′ end of the aminoacyl-tRNA substrate.

The region between 2058 and 2062 of the peptidyl-transferase loop is an area of diverse reactivity changes for many antibiotics and is known to be conformationally labile. In the case of puromycin, there is strong protection of G2058 (G2084) in the halophiles but no effect at A2058 in *E. coli.* Differences in the chemical footprint of the streptogramin A drugs, bound to archaeal and bacterial ribosomes, have also been observed at this position (Rodriguez-Fonseca et al., 1995; Porse & Garrett, 1999). In the presence of pristinamycin IIA, protection at G2058 (G2084) is observed in *Halobacteria halobium*, whereas enhancements are seen at A2058 in *Bacillus megaterium*, both in vitro and in vivo (Porse & Garrett, 1999). The conformational flexibility of this region is underscored by the variable weak effects at position 2062 that were observed in *E. coli* and *Hf. gibbonsii* in the presence of puromycin.

A working model called the streptogramin motif has been proposed based on footprinting and mutagenesis data (Porse & Garrett, 1999). The model juxtaposes the upper (2058–2062) and lower (2500–2506) regions of the peptidyl-transferase center, that are linked in many antibiotic footprints, in an irregular helix. The model includes A2060•G2505 and G2061•U2504 base pairings that are supported by several lines of mutagenesis evidence (see Porse & Garrett, 1999). Another feature of the model is that U2506 can form base pairs with either A/G2058 or A2059. Thus, the differences in the footprints between the two organisms may reflect two alternative, and perhaps functional, RNA conformers in this region.

The puromycin footprint obtained in *Hf. gibbonsii* ribosomes is similar to that obtained with pristinamycin IA complexed to *H. halobium* ribosomes (Porse & Garrett, 1999). Identical effects include an enhancement at 2503 and protections at 2058 and 2505. In addition, protection of position 2062 is a common feature if the

weak puromycin effect on *Hf. gibbonsii* ribosomes is included. Furthermore, there is a correspondence between the enhancement at position A2439 by pristinamycin IA in *H. halobium* and by puromycin in *E. coli*. The common effects of these drugs may be explained by the drugs inducing the same conformational change within the rRNA, perhaps in the context of the streptogramin motif described above. The only differences between the two drug footprints at the peptidyl-transferase center are the puromycin protection at G2553 and the pristinamycin IA effects at U2585 (protection) and A2059 (enhancement).

No enhancement effects were common to both *E. coli* and *Hf. gibbonsii*. An enhancement detected at A2521 in the halophile ribosomes corresponds to the modified m^2A2503 in *E. coli* (Kowalak et al., 1995). The latter modified nucleotide produces a weak primer extension stop (Fig. 2D) that precludes the observation of altered nucleotide reactivity, in the *E. coli* 23S rRNA, in the presence of DMS. A second enhancement at A2439 was only observed in *E. coli* ribosomes, neighboring the site in which the U2438A and U2438C mutations produced amicetin resistance in *H. halobium* (Leviev et al., 1994). These mutations caused a disruption in the local conformation because the reactivities of both A2439 and A2071 were enhanced in each of the mutants. In the same study, amicetin protected position A2070 in *E. coli*. Thus, the puromycin-induced effect at A2439 observed in *E. coli* may reflect weaker base stacking of the bulged loop nucleotides on the A2070-U2440 base pair in *E. coli* compared with the G-C base pair in the halophile.

In *E. coli*, enhancement effects were also observed outside the peptidyl-transferase center in domains I and III, at positions 508 and 1579, respectively. A new model of the three-dimensional arrangement of 23S rRNA within the 50S subunit is currently emerging from fitting the RNA to maps derived from cryo-electron microscopy using crosslinking, footprinting, and mutagenesis data from several laboratories (Müller et al., 2000). This model of 23S rRNA places nt 508 and 1579 in the lower back portion of the subunit and away from the peptidyl-transferase center. Nucleotide 508 is in a flexible loop connecting helices 2 and 24, whereas nt 1579 lies in helix 54. Importantly, both sites directly border the exit site of the nascent peptide.

The effects at A508 and A1579 may be because of (1) an allosteric effect transmitted along the peptide channel; (2) the presence of a secondary puromycin binding site that may or may not have functional relevance; or (3) peptidyl-puromycin release along the peptide channel. We favor explanation (1), the allosteric effect, for the following reasons. First, any binding of puromycin to a secondary ribosomal site is very weak and would probably not yield a footprint (Bourd et al., 1983). Second, although both nucleotides lie close to the peptide exit site (Müller et al., 2000), as a major effort was made to prepare 70S ribosomes and 50S subunits that were free of peptidyl-tRNA (Mahkno et al., 1988), the identities and relative yields of all the nucleotide protections and enhancements were unaltered for *E. coli* 70S ribosomes, 50S subunits, and polysomes. This renders it very unlikely that the A508 and A1579 effects are the result of puromycin-mediated peptide release along the peptide channel in our experiments. However, such a process could explain the earlier puzzling result, obtained in more crudely prepared ribosomes, of a direct crosslink of [^{3}H]-*p*-azidopuromycin to L23 (Nicholson et al., 1982a), which directly borders A508 and A1579 at the peptide-exit site (Fig. 6B).

Puromycin perturbs the position of the 3′ end of a deacylated tRNA substrate bound in the P-site, leading to strong reductions in the tRNA crosslinks to F2′ and F4′. Other peptidyl-transferase antibiotics also affect the yields of crosslinking, but only chloramphenicol and pristinamycin IIA produce such dramatic, albeit differing, effects (Kirillov et al., 1999). Pristinamycin IIA abolished the F2′ and F4′ crosslinks and reduced the crosslink to F1′, whereas chloramphenicol selectively abolished F2′. Therefore, most of the peptidyl-transferase drugs, including those previously assigned to the A-site, directly affect the positioning of the 3′ end of P′-site-bound tRNA.

Because puromycin is considered to be a structural analog of the 3′ end of an aminoacyl-tRNA substrate, it is reasonable to expect that there might be some correlation between the chemical footprints of puromycin and that of a tRNA substrate bound in the ribosomal A site. Removal of the 3′-terminal adenosine from yeast $tRNA^{Phe}$, although not from *E. coli* $tRNA^{Phe}$, bound in the presence of P-site-bound deacylated tRNA, resulted in increased modification of G2553 on *E. coli* ribosomes (unpubl. data cited in Moazed & Noller, 1989). Moreover, removal of the acyl moiety led to increased reactivities of Ψ2555, A2602, and U2609 in *E. coli* 23S rRNA (Moazed & Noller, 1989). Although G2553 is protected by puromycin, none of the other nucleotides are affected. This may reflect the fact that puromycin includes adenosine and 3′-linked aminoacyl moieties (Fig. 1), rather than a tRNA population containing a mixture of 2′- and 3′-linked aminoacyl groups in rapid equilibration via acyl transfer (Symons et al., 1978; Moazed & Noller, 1989).

Little is known about the molecular specificity of puromycin interactions with the ribosome. It is unlikely to be from base pairing because the analogs, 1-N^6-ethenoadenosine-Phe (Chladek et al., 1976), inosine-L-Phe, cytidine-L-Phe, and 3-N^4-ethenocytidine-Phe (Rychlik et al., 1970), are all effective acceptor substrates. It is more likely that weaker interactions occur within the rRNA, including base stacking.

In conclusion, the most likely puromycin-interaction sites are in the region of 2502–2506 of the peptidyl-transferase loop and in the terminal loop containing

G2553 (Fig. 9). Given that puromycin can act as a structural analog of an aminoacyl-tRNA substrate, both of these RNA regions must be closely juxtaposed at the catalytic center. Evidence supporting this hypothesis not only includes the common protections at G2505 and G2553 in bacteria and archaea, but also the strongly enhanced reactivity at A2503 (A2521) in the halophile that would have remained undetected in the *E. coli* 23S rRNA. Moreover, the effects of puromycin on the F2′ crosslink of deacylated ($2N_3$A76)tRNA at U2506 and on the putative UV-induced crosslinking yields of pristinamycin IA at m^2A2503/Ψ2504 further support the binding of puromycin to this putative "streptogramin motif" of the peptidyl-transferase loop (Fig. 9). In addition, these results correlate directly with the earlier finding that G2502 and U2504 are the principal crosslinking sites of *p*-azidopuromycin with rRNA (Hall et al., 1988).

MATERIALS and METHODS

Preparation of ribosomes

Tight-couple ribosomes and 50S subunits were prepared from *E. coli* MRE 600 as described (Makhno et al., 1988), except that particles were harvested at all preparative steps by centrifugation in a fixed angle rotor at 100,000 × *g*. The Makhno et al. (1988) procedure aims to remove endogenous mRNA and peptidyl-tRNA through dissociation of the ribosomes into subparticles, followed by reassociation. Briefly, tight-couple ribosomes, defined as those that remain associated between 4–6 mM Mg^{2+}, are initially purified in an associated state. The complexes are heated at 37 °C for 15 min in 3 mM $MgCl_2$ and 300 mM NH_4Cl, followed by sedimentation in a sucrose gradient to dissociate the particles into subunits. Equimolar amounts of subunits are then combined and subjected to repeated sedimentation in the above buffer used for isolation of purified 30S and 50S subunits. Alternatively, they are resedimented through a sucrose gradient in 5 mM $MgCl_2$ and 50 mM NH_4Cl for final selection of tight-couple 70S ribosomes. Polysomes were isolated essentially as described by Powers and Noller (1991).

Hf. gibbonsii (ATCC 33959) and *Hf. mediterranei* (ATCC 33500) ribosomes were prepared from cells that were grown to $A_{660} = 0.5$, spun down, and lysed by alumina grinding (1.5 g alumina/g cells) in high-salt buffer (20 mM Tris-HCl, pH 7.4, 60 mM magnesium acetate, 3 M KCl, and 6 mM 2-mercaptoethanol). The lysate was centrifuged at 15,000 rpm for 15 min in a Sorvall SS34 rotor. Because of the inactivation of DNAse I by the high salt concentration used, the DNA was pelleted by centrifugation at 45,000 rpm for 30 min. The supernatant from the second centrifugation was then recentrifuged at 48,000 rpm for 2.5 h in a Beckman Ti 65 rotor. The ribosomal pellet was gently resuspended with a glass rod and washed twice in high-salt buffer before repelleting by ultracentrifugation for 3 h at 45,000 rpm, and 15 h at 30,000 rpm. The ribosomes were clarified by centrifugation at 15,000 rpm for 10 min, divided into small aliquots and stored at −80 °C. All ribosomal preparations were highly active in poly(U)-dependent poly(Phe)-synthesis, where an assay optimized for halo archaea was used for both halophiles (Sanz et al., 1988).

RNA footprinting of puromycin-ribosome complexes

Puromycin-ribosome complexes were prepared as follows. Ribosomes (20 μg) were incubated at 30 °C for 20 min in 100 μL of the appropriate buffer (*E. coli*: 50 mM HEPES-KOH, pH 7.8, 10 mM $MgCl_2$, 15 mM KCl, 15 mM NH_4Cl, 1 mM DTT, and 0.1 mM EDTA; *Hf. gibbonsii* and *Hf. mediterranei*: 70 mM HEPES-KOH, pH 7.8, 60 mM magnesium acetate, 3 M KCl, and 6 mM 2-mercaptoethanol). Puromycin (Sigma) was then added to a final concentration of 0.1, 0.5, 1, 2, or 4 mM, and the mixture was incubated at 30 °C for 30 min before cooling slowly and placing on ice. Aliquots of ribosomes and puromycin-ribosome complexes (100 μL) were then reacted with the following chemical probes as described earlier (Christiansen et al., 1990): 1 μL DMS (1:1 dilution in ethanol), 5 μL kethoxal (35 mg/mL in 20% ethanol), and 100 μL CMCT (42 mg/mL in the appropriate buffer). For the DMS and kethoxal reactions, samples were incubated at 30 °C for 10 min, and the CMCT reaction mixture was incubated at 30 °C for 20 min. Reactions were stopped by standard procedures (Christiansen et al., 1990), and the RNA was precipitated by ethanol. Modified sites were identified by extension from ^{32}P-end-labeled oligodeoxynucleotide primers using reverse transcriptase (Life Sciences, Florida). The primers were hybridized to sites localized 150–200 nt apart along each 23S rRNA. Altered nucleotide reactivities were quantified by microdensitometry (Hoeffer, California). Autoradiograms were scanned and peak heights and areas determined. The total intensity change at a particular nucleotide position was calculated from the peak heights with a subtracted baseline correction for each peak.

The criteria for evaluating the significance of the footprinting results included the following: (1) reproducible observation of the effects in several different sets of experiments; (2) for *E. coli*, identical effects were observed for 70S ribosomes, 50S subunits, and polysomes; (3) the halophile effects were observed for two different organisms: *Hf. gibbonsii* and *Hf. mediterranei*; (4) the effects considered to be significant had a minimum total intensity change of 25–30%, whereas weaker total intensity changes were not accepted as significant; and (5) minor variations in the intensities of certain peaks observed from experiment to experiment were judged to be insignificant.

Binding and crosslinking of tRNA to ribosomes

The 2-azidoadenosine tRNA substrates and the poly (U) templates were prepared as described previously (Kirillov et al., 1999, and references therein). Tight-couple 70S ribosomes (2 μM) were incubated with poly (U) (1 μg/pmol ribosomes) in 20 mM Tris-Cl (pH 7.5), 50 mM NH_4Cl, 10 mM $MgCl_2$, and 0.5 mM EDTA for 5 min at 37 °C. Puromycin (1 mM) was added and incubated for 5 min at 37 °C before adding the azido-tRNA derivative at molar ratios of 0.5–1.1 and incubating another 30 min at 37 °C. The level of tRNA

binding was measured by nitrocellulose filter binding as described earlier (Kirillov et al., 1999). Crosslinks were generated by diluting the samples in cold buffer, and irradiating with 365 nM light at 0 °C, at a distance of 5 cm from the UV source. Analysis of the crosslinking products, including preparation of the rRNA fragments F1′, F2′, and F4′ by oligonucleotide-directed RNase H digestion, is detailed in Kirillov et al. (1999).

Interaction of PIA with 70S ribosomes

Pristinamycin IA (10 μM) was incubated with 70S ribosomes (150 nM) in 20 mM Tris-chloride, pH 7.5, 50 mM NH_4Cl, and 10 mM $MgCl_2$ at 37 °C for 10 min. Where indicated, deacylated tRNA (1.2 mol/mol ribosomes) was included in the presence of poly(U) (1 μg/pmol ribosomes). Puromycin (1 mM) was added either to preformed PIA–ribosome complexes or directly to 70S ribosomes before adding PIA. Following addition of puromycin or PIA, the samples were incubated at 37 °C for 10 min. Samples were maintained as droplets on a microtiter tray, placed on an ice-water bath, and subjected to UV irradiation in a Stratalinker 1800 (5 × 8 W bulbs, Stratagene, California) for 20 min at 365 nM. Samples were extracted with phenol, (1:1) phenol:chloroform, and chloroform, prior to ethanol precipitation to remove protein and antibiotics. The rRNA was subjected to primer extension using AMV reverse transcriptase (Life Sciences, Florida) and deoxyoligonucleotide primers complementary to rRNA 3′ to the modifications. The extension products were separated on denaturing polyacrylamide gels and autoradiographed.

ACKNOWLEDGMENTS

The research and B.T. Porse were supported by grants from the Danish Natural Science Research Council and the Danish Biotek II program. C. Rodriguez-Fonseca was a fellow of the Comunidad de Madrid and received EMBO short-term fellowships and a Danish Research Academy studentship. K.S. Long received an investigator fellowship from the Alfred Benzon Foundation. Richard Brimacombe is thanked for helpful discussions on the peptide exit site.

Received January 14, 2000; returned for revision February 25, 2000; revised manuscript received March 16, 2000

REFERENCES

Bocchetta M, Xiong L, Mankin AS. 1998. 23S rRNA positions essential for tRNA binding in ribosomal functional sites. *Proc Natl Acad Sci USA 95*:3525–3530.

Bourd SB, Kukhanova MK, Gottikh BP, Krayevsky AA. 1983. Cooperative effects in the peptidyl transferase center of *Escherichia coli* ribosomes. *Eur J Biochem 135*:465–469.

Chladek S, Ringer D, Abraham EM. 1976. Fluorescent 2′(3′)-O-aminoacylnucleosides-acceptor substrates for ribosomal peptidyltransferase+. *Nucleic Acids Res 3*:1215–1224.

Christiansen J, Egebjerg J, Larsen N, Garrett RA. 1990. Analysis of RNA structure: Experimental and theoretical considerations. In: Spedding G, ed. *Ribosomes and protein synthesis: A practical approach*. Oxford: Oxford University Press. pp 229–252.

Egebjerg J, Christiansen J, Garrett RA. 1991. Attachment sites of primary binding proteins L1, L2, and L23 on 23S ribosomal RNA of *Escherichia coli*. *J Mol Biol 222*:251–264.

Egebjerg J, Larsen N, Garrett RA. 1990. Structural map of 23S rRNA. In: Hill W, Dahlberg A, Garrett RA, Moore PB Schlessinger D, Warner J, eds. *The ribosome: Structure, function, and evolution*. Washington, DC: American Society for Microbiology Press. pp 168–179.

Egebjerg J, Leffers H, Christensen A, Andersen H, Garrett RA. 1987. Structure and accessibility of domain I of *E. coli* 23S rRNA in free RNA, in the L24 RNA complex and in 50S subunits: Implications for ribosomal assembly. *J Mol Biol 196*:125–136.

Fernandez-Muñoz R, Vázquez D. 1973. Binding of puromycin to *E. coli* ribosomes. Effects of puromycin analogues and peptide bond formation inhibitors. *Mol Biol Rep 1*:27–32.

Gale EF, Cundliffe E, Reynolds PE, Richmond RA, Waring MJ, eds. 1981. Antibiotic inhibitors of ribosome function. In: *The molecular basis of antibiotic action*. London: Wiley & Sons, Ltd. pp 402–457.

Garrett RA, Rodriguez-Fonseca C. 1995. The peptidyl transferase center. In: Zimmermann RA, Dahlberg A, eds. *Ribosomal RNA: Structure, evolution, processing and function*. Boca Raton, Florida: CRC Press. pp 327–355.

Green R, Switzer C, Noller HF. 1998. Ribosome-catalyzed peptide-bond formation with an A-site substrate covalently linked to 23S ribosomal RNA. *Science 280*:286–289.

Hall CC, Johnson D, Cooperman BS. 1988. [^{3}H]-*p*-Azidopuromycin photoaffinity labeling of *Escherichia coli* ribosomes: Evidence for site-specific interaction at U-2504 and G-2502 in domain V of 23S ribosomal RNA. *Biochem*istry *27*:3983–3990.

Harris RJ, Symons RH. 1973. On the molecular mechanism of action of certain substrates and inhibitors of ribosomal peptidyltransferase. *Bioorg Chem 2*:266–285.

Kim DF, Green R. 1999. Base-pairing between 23S rRNA and tRNA in the ribosomal A site. *Mol Cell 4*:859–864.

Kirillov S, Porse B, Vester B, Woolley P, Garrett RA. 1997. Movement of the 3′-end of tRNA through the peptidyl transferase center and its inhibition by antibiotics. *FEBS Lett 406*:223–233.

Kirillov SV, Porse BT, Garrett RA. 1999. Peptidyl transferase antibiotics perturb the relative positioning of the 3′-terminal adenosine of P/P′-site-bound tRNA and 23S rRNA in the ribosome. *RNA 5*:1003–1013.

Kowalak JA, Bruenger E, McCloskey JA. 1995. Posttranscriptional modification of the central loop of domain V in *Escherichia coli* 23S ribosomal RNA. *J Biol Chem 270*:17758–17764.

Leviev IG, Rodriguez-Fonseca C, Phan H, Garrett RA, Heilek G, Noller HF, Mankin AS. 1994. A conserved secondary structural motif in 23S rRNA defines the site of interaction of amicetin, a universal inhibitor of peptide bond formation. *EMBO J 13*:1682–1686.

Makhno VI, Peshin NN, Semenkov YP, Kirillov SV. 1988. Modified procedure of producing "tight" 70S ribosomes from *E. coli*, highly active in individual stages of the elongation cycle. *Mol Biol 22*: 528–537.

Moazed D, Noller HF. 1987. Chloramphenicol, erythromycin, carbomycin, and vernamycin B protect overlapping sites in the peptidyl transferase region of 23S rRNA. *Biochimie 69*:879–884.

Moazed D, Noller HF. 1989. Interaction of tRNA with 23S rRNA in the ribosomal A, P, and E sites. *Cell 57*:585–597.

Müller F, Sommer I, Baranov P, Stark H, van Heel M, Rodnina M, Wintermeyer W, Brimacombe R. 2000. The 3D arrangement of the RNA in the *E. coli* 50S ribosomal subunit. II. Distribution of functionally important sites. *J Mol Biol*. In press.

Nicholson AW, Hall CC, Strycharz WA, Cooperman BS. 1982a. Photoaffinity labeling of *Escherichia coli* ribosomes by an aryl azide analogue of puromycin. On the identification of the major covalently labeled ribosomal proteins and on the mechanism of photoincorporation. *Biochemistry 21*:3797–3808.

Nicholson AW, Hall CC, Strycharz WA, Cooperman BS. 1982b. Photoaffinity labeling of *Escherichia coli* ribosomes by an aryl azide analogue of puromycin. Evidence for the functional site specificity of labeling. *Biochemistry 21*:3809–3817.

Odom OW, Picking WD, Hardesty B. 1990. Movement of tRNA but not the nascent peptide during peptide bond formation on the ribosome. *Biochemistry 29*:10734–10744.

Pestka S. 1970. Studies on the formation of transfer ribonucleic acid-ribosome complexes. 8. Survey of the effect of antibiotics on

N-acetyl-phenylalanyl-puromycin formation: Possible mechanism of chloramphenicol action. *Arch Biochem Biophys 136*:80–88.
Pestka S. 1977. Inhibitors of protein synthesis. In: Weissbach H, Pestka S, eds. *Molecular mechanisms of protein biosynthesis*. New York: Academic Press. pp 467–553.
Porse BT, Garrett RA. 1995. Mapping important nucleotides in the peptidyl transferase center of 23S rRNA using a random mutagenesis approach. *J Mol Biol 249*:1–20.
Porse BT, Rodriguez-Fonseca C, Leviev I, Garrett RA. 1995. Antibiotic inhibition of the movement of tRNA substrates through a peptidyl transferase cavity. *Biochem Cell Biol 73*:877–885.
Porse BT, Garrett RA. 1999. Sites of interaction of streptogramin A and B antibiotics in the peptidyl transferase loop of 23S rRNA and the synergism of their inhibitory mechanisms. *J Mol Biol 286*: 375–387.
Porse BT, Kirillov SV, Awayez MJ, Garrett RA. 1999a. UV-induced modifications in the peptidyl transferase loop of 23S rRNA dependent on binding of the streptogramin B antibiotic, pristinamycin IA. *RNA 5*:585–595.
Porse BT, Kirillov SV, Awayez MJ, Ottenheijm HCJ, Garrett RA. 1999b. Direct crosslinking of the antitumor antibiotic sparsomycin, and its derivatives, to A2602 in the peptidyl transferase center of 23S-like rRNA within ribosome-tRNA complexes. *Proc Natl Acad Sci USA 96*:9003–9008.
Porse BT, Kirillov SV, Garrett RA. 2000. Antibiotics and the peptidyltransferase center. In: Garrett RA, Douthwaite SR, Liljas A, Matheson AT, Moore PB, Noller HF, eds. *The ribosome: Structure, function, antibiotics, and cellular interactions*. Washington, DC: American Society for Microbiology Press. pp 441–449.
Powers T, Noller HF. 1991. A functional pseudoknot in 16S rRNA. *EMBO J 10*:2203–2214.
Rodriguez-Fonseca C, Amils R, Garrett RA. 1995. Fine structure of the peptidyl transferase center on 23S-like rRNAs deduced from chemical probing of antibiotic-ribosome complexes. *J Mol Biol 247*:224–235.
Rychlik I, Cerna J, Chladek S, Pulkrabek P, Zemlicka J. 1970. Substrate specificity of ribosomal peptidyltransferase. The effect of the nature of the amino acid side chain on the acceptor activity of 2′(3′)-O-aminoacyladenosines. *Eur J Biochem 16*:136–142.
Sanz JL, Marín I, Balboa MA, Ureña D, Amils R. 1988. An NH_4^+ dependent protein synthesis cell-free system for halobacteria. *Biochemistry 27*:8194–8199.
Sanz JL, Marín I, Ureña D, Amils R. 1993. Functional analysis of seven ribosomal systems from extreme halophilic archaea. *Can J Microbiol 39*:311–317.
Smith JD, Traut RR, Blackburn GM, Monro RE. 1965. Action of puromycin in polyadenylic acid-directed polylysine synthesis. *J Mol Biol 13*:617–628.
Smith JE, Cooperman BS, Mitchell P. 1992. Methylation sites in *Escherichia coli* rRNA: Localization and identification of four new sites of methylation in 23S rRNA. *Biochemistry 31*:10825–10834.
Symons RH, Harris RJ, Greenwell P, Eckermann DJ, Vanin EF. 1978. The use of puromycin analogs and related compounds to probe the active center of peptidyl transferase on *Escherichia coli* ribosomes. *Bioorg Chem* (Suppl.) *4*:409–436.
Traut RR, Monro RE. 1964. The puromycin reaction and its relationship to protein synthesis. *J Mol Biol 10*:63–72.
Vázquez D. 1979. Inhibitors of protein synthesis. Berlin: Springer-Verlag.
Wower J, Wower IK, Kirillov SV, Rosen KV, Hixon SS, Zimmermann RA. 1995. Peptidyl transferase and beyond. *Biochem Cell Biol 73*:1041–1047.